Robust Rigid Shape Registration Method Using a Level Set Formulation

Muayed S. Al-Huseiny, Sasan Mahmoodi, and Mark S. Nixon

University of Southampton, School of Electronics and Computer Science, UK
{mssah07r,sm3,msn}@ecs.soton.ac.uk

Abstract. This paper presents a fast algorithm for robust registration of shapes implicitly represented by signed distance functions(SDFs). The proposed algorithm aims to recover the transformation parameters(scaling, rotation, and translation) by minimizing the dissimilarity between two shapes. To achieve a robust and fast algorithm, linear orthogonal transformations are employed to minimize the dissimilarity measures. The algorithm is applied to various shape registration problems, to address issues such as topological invariance, shape complexity, and convergence speed and stability. The outcomes are compared with other state-of-the-art shape registration algorithms to show the advantages of the new technique.

1 Introduction

Shape registration can be viewed as the result of a point-wise transformation between an observation and a reference shape. It is a fundamental task used to match two or more shapes taken, for example, at different times, from different viewpoints, or from different scenes. Virtually all large systems which evaluate images require the registration or a closely related operation as an intermediate step [1]. Shape registration is an essential requirement shared among many computer vision domains and applications, such as, pattern recognition, remote sensing, medical image analysis, and computer graphics to name a few.

The quality of registration is controlled using a similarity/dissimilarity measure. Also, the representation of the shape plays a crucial role in the registration process, and can significantly influence the overall performance of the registration algorithm. Active contours[2], Fourier descriptors[3] and active shapes models[4] are among the methods using explicit representations to describe arbitrary shapes. Although, these representations are powerful enough to capture a certain number of local deformations, they require a large number of parameters to deal with important shape deformations[5]. Non-parametric shape representations such as the signed distance functions(SDFs), are becoming a more popular choice, due to their implicit handling of various shape topologies , and the simple extension to describe higher dimensions than curves and surfaces[5].

Contour-based registration methods [6,7] are among the techniques used widely in shape registration, due to their fast convergence. These techniques however require point correspondence for the boundary of the shapes. However,

G. Bebis et al. (Eds.): ISVC 2010, Part II, LNCS 6454, pp. 252–261, 2010.

contour-based methods fall short, if two shapes to be registered have different Euler numbers.

Gradient descent-based registration techniques [5,8,9] widely used with segmentation applications are mostly characterized by low speed due to their iterative nature, instability and convergence to local minima, difficulty in implementation due to the need to tune the time step and stopping parameters for each transformation, and the limited extent of transformations these techniques can handle.

This paper presents a level set based shape registration algorithm. The algorithm proposed here employs linear transformation and shape moments to compute the parameters individually. We show that the registration technique presented here is robust, fast, and suitable for a wide range of registration problems with shapes' complexities. The results presented here are compared with state-of-the-art registration algorithms in the literature.

In the rest of the paper, we state the transformation problem in section 2, describe the proposed algorithm in section 3, present the experimental results in section 4, and conclude the paper in section 5.

2 The Statement of the Problem

Let $\phi_p(x,y) : \Omega \rightarrow \Re$ and $\phi_q(x,y) : \Omega \rightarrow \Re$ denote Lipschitz functions representing SDFs of shapes $p(x,y)$ and $q(x,y)$. These functions are defined as,

$$\phi_P(x,y) = \left\{ \begin{array}{ll} D_E((x,y),P), & (x,y) \in I_P, \\ -D_E((x,y),P), & (x,y) \in \Omega - I_P, \end{array} \right\} \tag{1}$$

where D_E represents the minimum Euclidean distance between the shape boundary I_P and each point in the domain Ω.

Parameters s, θ, T_x and T_y representing scaling, rotation, and translations in x and y directions respectively are required to transform ϕ_q to minimize the distance between ϕ_p and the transformed ϕ_q, i.e.:

$$(\hat{\theta}, \hat{s}, \hat{T}_x, \hat{T}_x) = \underset{\boldsymbol{\theta}, \boldsymbol{s}, \boldsymbol{T_x}, \boldsymbol{T_y}}{\operatorname{argmin}} \int\int |\phi_p(x,y) - \phi_q(sR_\theta(x+T_x, y+T_y))|^2 \, \mathrm{d}x\mathrm{d}y. \tag{2}$$

where,

$$R_\theta = \begin{bmatrix} \cos\theta & -\sin\theta \\ \sin\theta & \cos\theta \end{bmatrix}.$$

The minimization of Eq.2 leads to a set of non-linear equations with respect to the desired parameters as discussed in [5]. The algorithm minimizing the distance measure (2) is slow to converge, can fall into local minima and requires continuously tuned parameters for smooth convergence [8]. The objective of this paper is therefore to propose a robust algorithm minimizing (2) and avoiding local minima with fast convergence, and no requirement for parameter tuning.

3 Shape Registration

3.1 Rotation

In order to find the optimal angle for rotation we conveniently employ polar coordinates. We use the notion that a rotation in Cartesian domain is displacement in polar domain [10]. Here we employ the translation invariance of the shapes' SDFs,

$$\hat{\phi}_p(x,y) = \phi_p(x - p_x, y - p_y), \tag{3}$$

$$\hat{\phi}_q(x,y) = \phi_q(x - q_x, y - q_y), \tag{4}$$

where (p_x, p_y) and (q_x, q_y) are respectively the centroids of ϕ_p and ϕ_q. A simple and efficient algorithm[11] is used to map $\hat{\phi}_p(x,y)$ and $\hat{\phi}_q(x,y)$ to polar coordinates, to obtain $\hat{\phi}_p(\rho,\omega)$ and $\hat{\phi}_q(\rho,\omega)$, so that: $x = \rho\cos\omega$, and $y = \rho\sin\omega$. These $2D$ centralized SDFs contain some redundancy in terms of their radial parameterization ρ which has no impact on the angle difference between the two SDFs. In order to remove the dependency of $\hat{\phi}_p(\rho,\omega)$ and $\hat{\phi}_q(\rho,\omega)$ on ρ, we integrate $\hat{\phi}_p(\rho,\omega)$ and $\hat{\phi}_q(\rho,\omega)$ with respect to ρ according to (5) and (6) We also notice that this dependency removal of ρ increases the computational speed.

$$\tilde{\phi}_p(\omega) = \int_\rho \hat{\phi}_p(\rho,\omega)\mathrm{d}\rho, \tag{5}$$

$$\tilde{\phi}_q(\omega) = \int_\rho \hat{\phi}_q(\rho,\omega)\mathrm{d}\rho. \tag{6}$$

Let $\bar{\phi}_p$ denote a normalized instance of $\hat{\phi}_p$, i.e.:

$$\bar{\phi}_p(\omega) = \frac{\hat{\phi}_p(\omega)}{\int_\omega \hat{\phi}_p(\omega)\mathrm{d}\omega}. \tag{7}$$

The unknown angle will be estimated by minimizing the dissimilarity measure in (8),

$$\begin{aligned}
\int_\omega \left|\tilde{\phi}_q - \beta\bar{\phi}_p\right|^2 \mathrm{d}\omega &= \int_\omega \left(\left|\tilde{\phi}_q - \beta\bar{\phi}_p\right|^T \left|\tilde{\phi}_q - \beta\bar{\phi}_p\right|\right)\mathrm{d}\omega, \\
&= \int_\omega \left((\tilde{\phi}_q)^T\tilde{\phi}_q - \beta(\tilde{\phi}_q)^T\bar{\phi}_p - \beta\tilde{\phi}_q(\bar{\phi}_p)^T + \beta^2(\bar{\phi}_p)^T\bar{\phi}_p\right)\mathrm{d}\omega, \\
&= \int_\omega \left(\left|\tilde{\phi}_q\right|^2 - 2\beta\left\langle\tilde{\phi}_q\cdot\bar{\phi}_p\right\rangle + \beta^2\left|\bar{\phi}_p\right|^2\right)\mathrm{d}\omega,
\end{aligned} \tag{8}$$

where β is defined as, $\beta := \left\langle\tilde{\phi}_q\cdot\bar{\phi}_p\right\rangle$.

Since $\left|\bar{\phi}_p\right|^2 = 1$ (Eq.7), we have,

$$\int_\omega \left|\tilde{\phi}_q - \beta\bar{\phi}_p\right|^2 \mathrm{d}\omega = \int_\omega \left|\tilde{\phi}_q\right|^2 \mathrm{d}\omega - \beta^2. \tag{9}$$

Hence the minimization of (8) is achieved by maximizing β. The optimal rotation angle is therefore calculated by finding θ that maximizes β, or,

$$\hat{\theta} = \underset{\boldsymbol{\theta}}{\operatorname{argmax}}\ \beta. \tag{10}$$

The maximum β is computed using the Fourier transform. Let the Fourier transform of $\hat{\phi}_q$ and $\bar{\phi}_p$ be respectively $\hat{\psi}_q(\xi)$ and $\bar{\psi}_p(\xi)$, such that,

$$\bar{\psi}_p(\xi) = \int_\xi \bar{\phi}_p(\omega) e^{-i(\omega\xi)2\pi} \mathrm{d}\omega. \tag{11}$$

$$\tilde{\psi}_q(\xi) = \int_\xi \tilde{\phi}_q(\omega) e^{-i(\omega\xi)2\pi} \mathrm{d}\omega, \tag{12}$$

Therefore, by using Parseval's theorem, we can write:

$$\begin{aligned}\beta(\theta) = \left\langle \tilde{\phi}_q(\omega) \cdot \bar{\phi}_p(\omega+\theta) \right\rangle &= \int_\omega \left(\tilde{\phi}_q(\omega)\bar{\phi}_p(\omega+\theta)\right) \mathrm{d}\omega \\ &= \int_\xi \left(\tilde{\psi}_q(\xi)\bar{\psi}_p^*(\xi) e^{i(\xi\theta)2\pi}\right) \mathrm{d}\xi,\end{aligned} \tag{13}$$

where $(*)$ denotes the complex conjugate. Hence, $\hat{\theta}$ is computed as:

$$\hat{\theta} = \underset{\boldsymbol{\theta}}{\operatorname{argmax}}\ \beta = \underset{\boldsymbol{\theta}}{\operatorname{argmax}} \int_\xi \left(\tilde{\psi}_q(\xi)\bar{\psi}_p^*(\xi) e^{i(\xi\theta)2\pi}\right) \mathrm{d}\xi. \tag{14}$$

3.2 Scale

We use the geometric moments of SDFs to characterize the shapes' features to calculate the scaling parameter. It can be shown that if one shape is a scaled version of another then the corresponding SDFs are proportional to the scale factor[5],

$$s\hat{\phi}_p(x,y) = \hat{\phi}_q(sx, sy), \tag{15}$$

where s is the scale parameter. The geometrical moments of the reference SDF $\hat{\phi}_p$ and the observed SDF $\hat{\phi}_q$ are computed as:

$$M_m^{\hat{q}} = \int\int \left(\sqrt{x^2+y^2}\right)^m\ \hat{\phi}_q(x,y)\mathrm{d}x\ \mathrm{d}y, \tag{16}$$

$$M_m^{\hat{p}} = \int\int \left(\sqrt{x^2+y^2}\right)^m\ \hat{\phi}_p(x,y)\mathrm{d}x\ \mathrm{d}y, \tag{17}$$

where m represents the degree of the moment. Substituting Eq.15 into Eq.17, we arrive at Eq.18:

$$M_m^{\hat{p}} = \frac{1}{s} \int\int \left(\sqrt{x^2+y^2}\right)^m \hat{\phi}_q(sx, sy)\, \mathrm{d}x\mathrm{d}y. \tag{18}$$

By changing variables, $X = sx$, and $Y = sy$, Eq.18 can be written as,

$$\begin{aligned} M_m^{\hat{p}} &= \int\int \frac{\left(\sqrt{X^2+Y^2}\right)^m}{s^m} \hat{\phi}_q(X,Y) \frac{\mathrm{d}X\ \mathrm{d}Y}{s^2}, \\ &= \frac{1}{s^{(m+3)}} \int\int \left(\sqrt{X^2+Y^2}\right)^m \hat{\phi}_q(X,Y) \mathrm{d}X\ \mathrm{d}Y, \\ &= \frac{1}{s^{(m+3)}} M_m^{\hat{q}}. \end{aligned} \tag{19}$$

Let E be the error defined in Eq.20:

$$E = \sum_m \left| M_m^{\hat{q}} - s^{m+3} M_m^{\hat{p}} \right|^2. \tag{20}$$

Since Eq.20 is non-linear with respect to variable s, with a change of variable, the above non-linear least squares problem is reduced to a linear one, i.e.:

$$\acute{E} = \sum_m \left| \log\left(\frac{M_m^{\hat{q}}}{M_m^{\hat{p}}}\right) - (m+3)\log s \right|^2. \tag{21}$$

Hence the optimal scale parameter $\hat{s}$ is estimated by minimizing $\acute{E}$:

$$\hat{s} = \underset{\boldsymbol{s}}{\operatorname{argmin}}\ \acute{E}. \tag{22}$$

It should be noted that the use of Chebyshev or Zernike moments leads to a non-linear least squares problem whose minimization is more difficult and demanding than the current method proposed here. In the case of Chebychev and Zernike moments, the non-linearity does not reduce to a linear problem by using a change of variables.

3.3 Translation

Using the scaling and rotation parameters calculated in 3.1 and 3.2, we optimize Eq.2 to calculate T_x and T_y:

$$\phi_p(x,y) = \phi_q(x - T_x, y - T_y). \tag{23}$$

By employing the same method explained in 3.1, the translation parameters are calculated as:

$$\begin{aligned} \left[\acute{T}_x\ \acute{T}_y\right] &= \underset{\boldsymbol{T_x},\boldsymbol{T_y}}{\operatorname{argmax}} \left\langle \phi_q, \check{\phi}_p \right\rangle, \\ &= \underset{\boldsymbol{T_x},\boldsymbol{T_y}}{\operatorname{argmax}} \int_{\omega_x}\int_{\omega_y} \left(\psi_q(\omega_x,\omega_y)\check{\psi}_p(\omega_x,\omega_y) e^{i(T_x\omega_x + T_y\omega_y)2\pi}\right) \mathrm{d}\omega_x \mathrm{d}\omega_y, \end{aligned} \tag{24}$$

where $\check{\phi}_p$ is a normalized instance of ϕ_p, $\acute{T}_x$ and $\acute{T}_y$ represent the estimated optimal translation parameters, $\psi_q(\omega_x, \omega_y)$ and $\check{\psi}_p(\omega_x, \omega_y)$ represent respectively the 2D Fourier transform of ϕ_q and $\check{\phi}_p$, and ω_x and ω_y are the spatial frequencies.

Remark: Since images in practice are in discrete domain, we employ Fast Fourier transform(FFT) instead of continuous Fourier transforms employed in this section. We are therefore required to modify the definition of SDFs to cope with the periodicity property imposed by FFT.

Let Ω be the image domain. This domain is partitioned by the shape perimeter into two regions, the shape interior (convex hull) I_P and the background, and let $\ddot{\phi} : I_P \rightarrow \Re^+$ be a Lipschitz function that represents the distance transform for the interior of the shape P. This is expressed in (25):

$$\ddot{\phi}_P(x,y) = \left\{ \begin{array}{ll} D_E((x,y),P), & (x,y) \in I_P, \\ 0, & (x,y) \in \Omega - I_P, \end{array} \right\} \tag{25}$$

This modified SDF representation is induced by the periodicity requirements of the FFT used in Section 3.

4 Results and Discussions

In the following we present a set of examples, each of which is intended to show the advantage of the shape registration method presented here over other known registration methods in a particular shape registration problem. For better demonstration, the figures show the contours of the observed and reference shapes before and after registration.

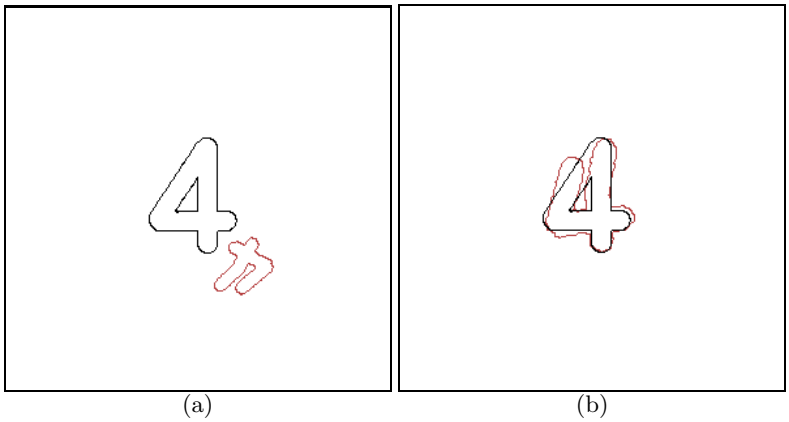

(a) (b)

Fig. 1. The registration of shapes with different topologies. (a)The observation is a transformed open '4' with Euler characteristic 1, while the reference is a closed one with Euler characteristic 0. (b)The two shapes superimposed optimally using the proposed approach.

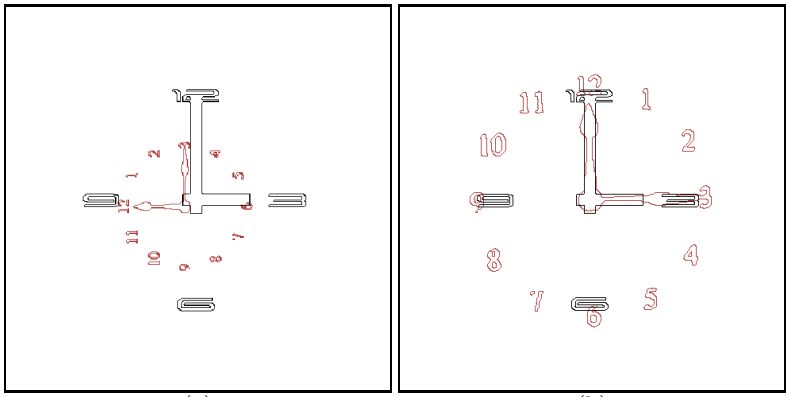

(a) (b)

Fig. 2. The registration of shapes with different number of shape components. (a)The reference shape has clock hands and compass point indicators, whereas the observed shape has smaller hands and more conventional indicators. (b)The result after applying our technique.

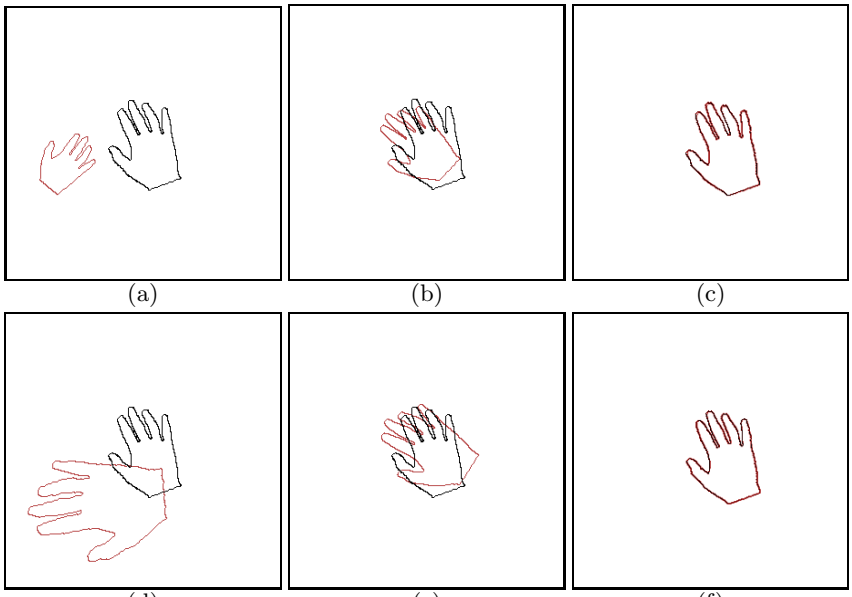

(a) (b) (c)

(d) (e) (f)

Fig. 3. The registration of identical shapes with synthetic transformations. (a and d) The observed shape is a replica of the reference shape with θ=-60, s=0.7, Tx=-90, Ty=20, and θ=75, s=1.5, Tx=-50, Ty=50 respectively. (b and e) The registration using gradient descent method [5], notice the inaccuracy of registration caused by the local minima issue. (c and f) The registration using the new method, the shapes are almost perfectly registered.

– **Contour Methods:**

In the first example we use two shapes with different Euler characteristics. Such shapes have completely different contours (topologies) and hence the contour based methods fail to calculate the correct transformation parameters, also it is hard to establish automatic contour points correspondences. In Figure 1, the observed shape is an open number four with Euler characteristic one, and the reference shape is a closed four with Euler characteristic zero. These shapes have different topologies, however they have been correctly registered using the registration approach proposed in this paper.

In the second example we register two complex shapes each having different number of components. The employment of contour methods to register such shapes for example by registering the individual objects in the observed shape to their counterparts in the reference shape may do partially, wherein the objects with no counterparts remain unregistered. In Figure 2 the observed shape is a clock face with conventional indicators while the reference shape has compass point indicators, this example demonstrates the registration algorithm proposed here can register two shapes, even if there is no one to one correspondence among components forming the shapes.

– **Gradient Descent Methods:**

In the third example we test a gradient descent based method proposed by Paragios *et al.*[5] using various transformation parameters. Figure 3 shows the local minima problem associated with these methods which leads to inaccurate

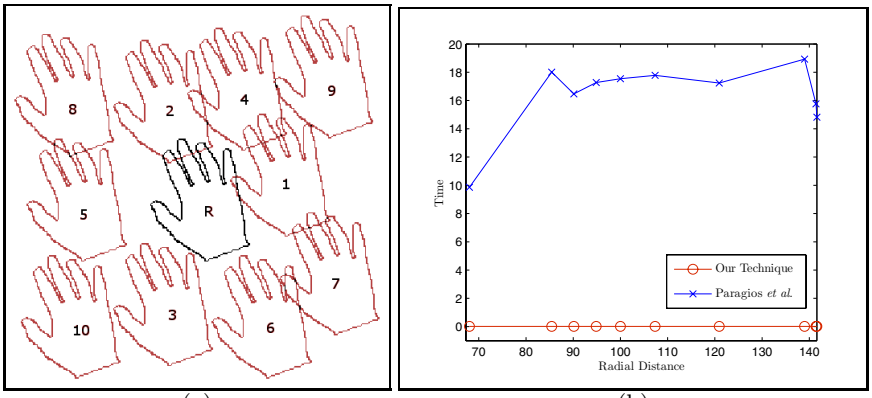

(a) (b)

Fig. 4. The registration of similar shapes with synthetic translations. (a) The observed shape is a replica of the reference shape R with ten different translations numbered ascendingly according to the radial distances from R. (b) A plot of the convergence time for each translation, it shows that the average convergence time for the gradient descent method is (16) seconds, while for our technique the average time is (0.012) seconds.

registration. In the figure, two different sets of transformation parameters are used to transform a shape and then gradient descent method is used to find these parameters. This is compared to the result of the same registration problem using our technique with two pass registration for more accuracy.

In the fourth example we study the issue of speed. The observed shape is a replica of the reference shape having the same rotation angle and scale. We employ ten randomly chosen translations for the observed shape. Both our algorithm and the gradient descent method cited in [5] are used to recover the translation parameters. The choice to test the convergence time for translation parameters is induced by the fact that translation is a linear transformation. Figure 4 shows the registration of the observed shape with ten arbitrarily chosen translations. The shapes are numbered according to their radial distance ($r = \sqrt{(x_r - x_o)^2 + (y_r - y_o)^2}$) to the reference shape, where (x_r, y_r) and (x_o, y_o) are respectively the center coordinates of the reference and the observed shapes. In Figure 4-(b), we plot the convergence time for both techniques against the radial distance r. From this plot we observe that the proposed method is faster and the speed is almost constant for all translations. The convergence time depends only on the size of the shape domain. The gradient descent method [5] on the other hand has variable speed of convergence. This depends on the actual translation and the magnitude of the gradient in each direction, such factors justify the non linear convergence time noticed in this figure.

5 Conclusions

This paper presents a shape registration algorithm which uses a modified signed distance function to represent the shapes. The proposed algorithm estimates the parameters using closed form expressions. This algorithm exploits Parseval's theorem to estimate the rotation and the translation parameters, and uses the geometric moments to estimate the scale parameters. The registration technique has been tested on shapes selected to demonstrate successful extraction and performance. Our method is robust in registering complex shapes and shapes with various topologies which can not be registered using contour based methods. The experimental results show that our registration algorithm is fast, accurate, stable, and does not fall into local minima.

Acknowledgment. This work was supported in part by the IST Programme of the European Community, under the PASCAL2 Network of Excellence, IST-2007-216886 and PinView Project, 216529. This publication only reflects the authors' views.

References

1. Brown, L.G.: A survey of image registration techniques. ACM Computing Surveys 24, 325–376 (1992)
2. Kass, M., Witkin, A., Terzopoulos, D.: Snakes: Active contour models. International Journal of Computer Vision 1, 321–331 (1988)

3. Zahn, C.T., Roskies, R.Z.: Fourier descriptors for plane closed curves. IEEE Transactions on Computers 21, 269–281 (1972)
4. Cootes, T.F., Taylor, C.J., Cooper, D.H., Graham, J.: Active shape models-their training and application. Computer Vision and Image Understanding 61, 38–59 (1995)
5. Paragios, N., Rousson, M., Ramesh, V.: Non-rigid registration using distance functions. Computer Vision and Image Understanding 89, 142–165 (2003)
6. Marques, J.S., Abrantes, A.J.: Shape alignment – optimal initial point and pose estimation. Pattern Recognition Letters 18, 49–53 (1997)
7. Markovsky, I., Mahmoodi, S.: Least-squares contour alignment. IEEE Signal Processing Letters 16, 41–44 (2009)
8. Cremers, D., Osher, S.J., Soatto, S.: Kernel density estimation and intrinsic alignment for shape priors in level set segmentation. International Journal of Computer Vision 69, 335–351 (2006)
9. Vemuri, B.C., Ye, J., Chen, Y., Leonard, C.M.: Image registration via level-set motion: applications to atlas-based segmentation. Medical Image Analysis 7, 1–20 (2003)
10. Casasent, D., Psaltis, D.: Position, rotation and scale invariant optical correlation. Applied Optics 15, 1795–1799 (1976)
11. Mukundan, R.: A comparative analysis of radial-tchebichef moments and zernike moments. In: British Machine Vision Conference 2009 (2009)